Role of the kinetochore/cell cycle checkpoint protein ZW10 in interphase cytoplasmic dynein function

Dileep Varma, Denis L. Dujardin, Stephanie A. Stehman, and Richard B. Vallee

Department of Pathology and Cell Biology, Columbia University, New York, NY 10032

Zeste white 10 (ZW10) is a mitotic checkpoint protein and the anchor for cytoplasmic dynein at mitotic kinetochores, though it is expressed throughout the cell cycle. We find that ZW10 localizes to pericentriolar membranous structures during interphase and cosediments with Golgi membranes. Dominant-negative ZW10, anti-ZW10 antibody, and ZW10 RNA interference (RNAi) caused Golgi dispersal. ZW10 RNAi also dispersed endosomes and lysosomes. Live imaging of Golgi, endosomal, and lysosomal markers after reduced ZW10 expression showed a specific decrease in the frequency of minus end–directed movements. Golgi membrane–associated dynein was markedly decreased, suggesting a role for ZW10 in dynein cargo binding during interphase. We also find ZW10 enriched at the leading edge of migrating fibroblasts, suggesting that ZW10 serves as a general regulator of dynein function throughout the cell cycle.

Introduction

Cytoplasmic dynein is responsible for the distribution and transport of diverse membranous organelles and is involved in chromosome segregation and mitotic spindle organization and orientation. Recent studies have also suggested a role for dynein in the removal of metaphase checkpoint proteins from the kinetochore (Howell et al., 2001; Wojcik et al., 2001) and in directed cell migration (Dujardin et al., 2003). The mechanisms by which dynein interacts with a diversity of cargoes and subcellular targeting sites is incompletely understood. The dynein intermediate, light intermediate, and light chains have each been implicated in cargo binding (for review see Vallee et al., 2004), as has another multisubunit complex, dynactin (Echeverri et al., 1996).

Zeste white 10 (ZW10) is a kinetochore protein that participates in the mitotic checkpoint and also serves to link dynactin and dynein to mitotic kinetochores (for review see Karess, 2005). *Drosophila melanogaster zw10*-null mutants exhibit chromosome missegregation and abnormal separation of sister chromatids in the presence of colchicine (Williams et al., 1992), a result confirmed by the injection of HeLa cells with anti-ZW10 antibody (Chan et al., 2000). *zw10*-null mutants also lack dynein at their kinetochores (Starr et al., 1998). ZW10 was found to interact with the dynactin subunit dynamitin (Starr et al., 1998), which, when overexpressed, had been found to displace the rest of the dynactin complex, along with cytoplasmic dynein, from kinetochores (Echeverri et al., 1996; Tai et al., 2002). ZW10 exists as a complex with *rough deal* (*rod*), *zwilch*, and the Rad50-interacting protein-1 (RINT-1; Scaerou et al., 1999, 2001; Basto et al., 2000; Chan et al., 2000; Savoian et al., 2000; Williams et al., 2003; Kops et al., 2005).

Despite clear evidence of a mitotic function, ZW10 is expressed uniformly throughout the cell cycle (Starr et al., 1997). Furthermore, its interacting partner dynamitin participates in general dynein function (Echeverri et al., 1996; Burkhardt et al., 1997). ZW10 has been reported to colocalize with the ER by immunocytochemistry and to participate in ER–Golgi trafficking through a SNARE-dependent mechanism (Hirose et al., 2004), although the specific role of ZW10 in this process was uncertain. This study was initiated to explore potential dynein-related activities of ZW10 during interphase. We report that ZW10 associates with specific interphase structures and regulates minus end–directed Golgi, endosome, and lysosome transport, which is consistent with a general role in dynein regulation and targeting.

D. Varma and D.L. Dujardin contributed equally to this paper.

Correspondence to Richard B. Vallee: rv2025@columbia.edu

D.L. Dujardin's present address is Ecole Supérieure de Biotechnologie de Strasbourg-Centre National de la Recherche Scientifique, UMR 7100, 67412 Illkirch Cedex, France.

Abbreviations used in this paper: β-COP, β-coatomer protein; NAGT, *N*-acetylglucosaminyltransferase; RINT-1, Rad50-interacting protein-1; RNAi, RNA interference; siRNA, small interfering RNA; shRNA, short hairpin RNA; ZW10, zeste white 10.

The online version of this article contains supplemental material.

The Journal of Cell Biology, Vol. 172, No. 5, February 27, 2006 655–662
http://www.jcb.org/cgi/doi/10.1083/jcb.200510120

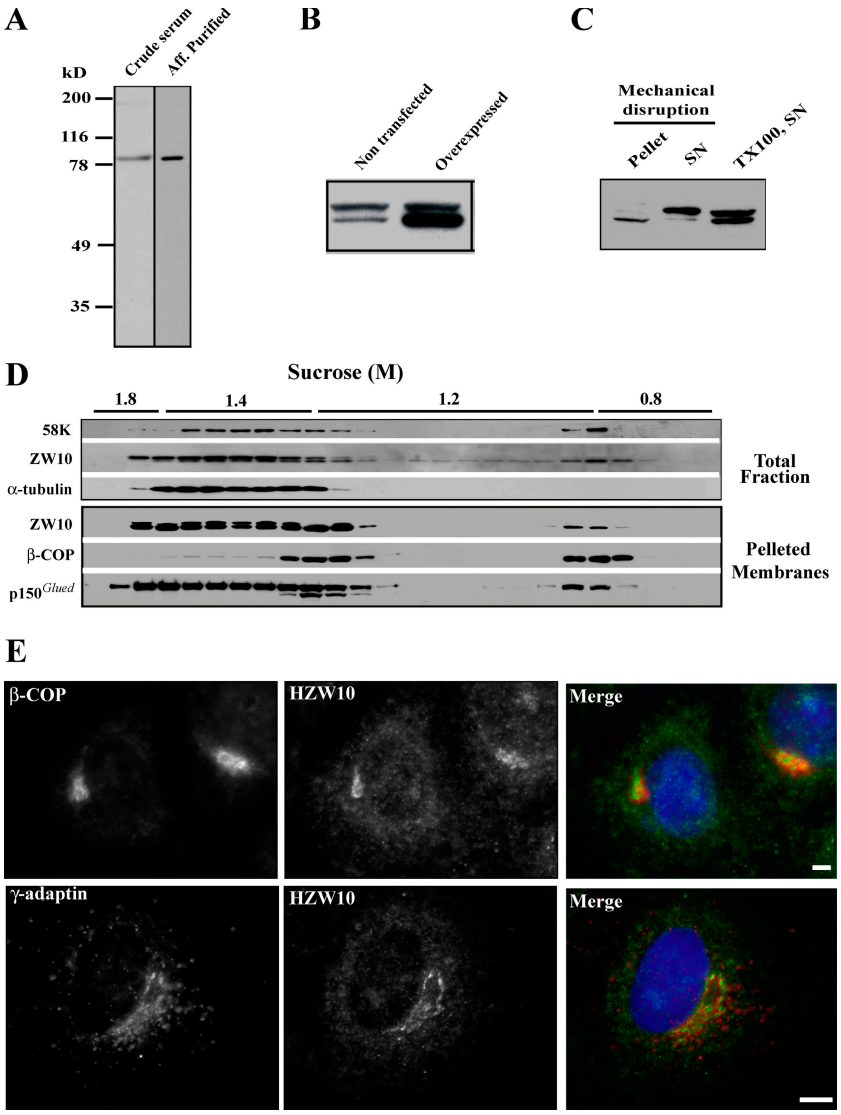

Figure 1. **Cofractionation and localization of ZW10 with Golgi membranes in interphase cells.** (A) Western blot of COS-7 cells with anti-Cter ZW10 peptide antibody. (B) Western blot of COS-7 cell extracts that were nontransfected or overexpressing full-length ZW10 probed with anti-HZW10 antibody (Starr et al., 1997). (C) Solubility of ZW10. ZW10 (B, bottom band) is sedimentable in lysates from mechanically disrupted cells (left and middle lanes), but remains in the supernatant from detergent-extracted cells (right lane). (D) Membrane flotation of postnuclear COS-7 extracts on a 0.8/2.0 M sucrose step gradient (Balch et al., 1984). Total protein (top) or pelleted membranes (bottom) from each fraction were subjected to Western blotting with a series of antibodies. ZW10 cofractionated with the Golgi markers 58K and β-COP, as well as with the dynactin subunit p150^{Glued}, at the 0.8/1.2 M sucrose interface. α-Tubulin and the upper band recognized by HZW10 antibody are present in the soluble fractions and absent from the 0.8/1.2 M sucrose interface. (E) Immunocytochemistry of ZW10. Deconvoluted projections of triple-labeled COS-7 cells showing elements of the Golgi apparatus (red, anti–β-COP and anti–γ-adaptin), ZW10 (green, anti-HZW10), and DNA (blue, DAPI). Bars, 5 μm.

Results and discussion

Association of ZW10 with membranous organelles

To examine the subcellular distribution of ZW10 in interphase cells, immunofluorescence microscopy was performed. A previously characterized antibody, "anti-HZW10," recognizes a doublet at the ZW10 position (Fig. 1 B; Starr et al., 1997), only the lower band of which is enhanced in cells expressing recombinant ZW10. An additional antibody produced against a COOH-terminal human ZW10 peptide, "anti-Cter," was specific for ZW10 (Fig. 1 A). Using either of the antibody punctates, pericentrosomal staining was generally observed in interphase cells (Fig. 1 E) that was absent in preimmune controls and was dispersed by brefeldin A or nocodazole (not depicted). Specific colocalization of ZW10 could be observed with the Golgi markers β-coatomer protein (β-COP), γ-adaptin (Fig. 1 E), 58K protein, and *N*-acetylglucosaminyltransferase (NAGT; not depicted), and additional ZW10-positive spots could be seen throughout the cell. Specific labeling of ER, endosomes, or lysosomes could not be discerned, as is the case with other dynein pathway components.

Consistent with a membrane association, ZW10 appeared primarily in the insoluble fraction in HeLa (Starr et al., 1997) and COS-7 cell extracts (Fig. 1 C, bottom band), but could be solubilized using a nonionic detergent (Fig. 1 C, TX100, SN). ZW10 was also enriched with Golgi membranes in subcellular fractionation studies (Fig. 1 D, top) and was separated from soluble markers, including the top 90-kD band recognized by the anti-HZW10 antibody (Fig. 1 B; Starr et al., 1997) and α-tubulin. The Golgi-associated ZW10 could be sedimented and solubilized with Triton X-100 (Fig. 1 D, bottom), which is consistent with a membrane association. The detection of ZW10 in other membrane flotation fractions (Fig. 1 D) supports an association with additional organelles as well.

Inhibition of ZW10 function

We used multiple approaches to inhibit ZW10 function. Overexpression of the COOH-terminal ZW10 fragment HZW10-4 produced a pronounced dominant-negative phenotype

(Fig. S1 A,available at http://www.jcb.org/cgi/content/full/jcb.200510120/DC1), though no effect was observed with other fragments or full-length ZW10. Mitotic index was dramatically reduced (0.5 ± 0.1 vs. 2.6 ± 0.3% for controls), even in the presence of nocodazole (0.2 ± 0.05 vs. 5.2 ± 0.1% for controls; Basto et al., 2000; Chan et al., 2000), and there was a substantial increase in multinucleate cells (23.5 ± 4.2 vs. 4.3 ± 0.6% in controls), many of which had micronuclei and/or unequally sized micronuclei (48.4%; Kops et al., 2005). HZW10-4 overexpression resulted in a marked increase in cells with a dispersed Golgi apparatus (68.4 ± 3.9 vs. 8.1 ± 3.3% for nonexpressing cells, and 12.9 ± 2.8% for high level β-galactosidase overexpressers as controls; Fig. S1, B and C).

Microinjection of COS-7 cells with affinity-purified anti-Cter ZW10 peptide antibody also caused Golgi dispersal (49 ± 3%; Fig. S2 A, top, available at http://www.jcb.org/cgi/content/full/jcb.200510120/DC1), compared with cells injected with peptide-blocked antibody (13.9 ± 4.6%; Fig. S2 A, bottom). Both HZW10-4–overexpressing and antibody-injected cells exhibited a substantial loss of centrosome-centered microtubule organization (Fig. S2 B, top), a result also produced by expression of dynamitin and other dynactin polypeptides (Burkhardt et al., 1997; Quintyne et al., 1999). To test whether Golgi dispersal is a direct or indirect effect of altered ZW10 function, we performed quadruple labeling using anti-tubulin, anti-58K, DAPI, and the injected anti-ZW10 antibody. For cells with clear Golgi dispersal, a normally centered microtubule organization was still detectable in 26.9 ± 1.8% of the cases (Fig. S2 B, bottom), indicating that the distribution of the Golgi is affected independently of microtubule defects in our experiments.

We also used RNA interference (RNAi) to inhibit ZW10 expression. ZW10 expression was greatly reduced after 3 d of ZW10 small interfering RNA (siRNA) treatment, whereas no reduction was detected after using a scrambled siRNA control (Fig. 2 A). Dynein and dynactin levels were unaffected by reduced ZW10 expression (Fig. 2 A). As for HZW10-4 overexpressers, ZW10 RNAi reduced mitotic index (2.1 ± 0.2%) versus control siRNA-treated cells (5.5 ± 0.3%; Kops et al., 2005). Cultures with reduced ZW10 also displayed a dramatic increase in Golgi dispersal, as visualized using the NAGT-GFP marker (49.3 ± 4.2% for ZW10 siRNA vs. 17.3 ± 2.3% for control siRNA; Fig. 2, B and C), which is similar to results obtained by Hirose et al. (2004) in HeLa cells. However, as observed for anti-Cter–injected cells (see previous paragraph), centrosome-centered microtubule organization was altered in many of the COS7 cells treated with ZW10 siRNA (Fig. 2 C, middle; 80% of the cells showed dispersed Golgi), but Golgi dispersal could still be observed in cells displaying a normally centered microtubule network (Fig. 2 C, bottom). We also transfected cells with a cDNA encoding a ZW10 short hairpin RNA (shRNA) corresponding to a target sequence distinct from that of the siRNA. Recipient cells again showed clear Golgi dispersal, as well as microtubule disruption (not depicted).

To gain insight into the basis for microtubule disruption, we examined the effects of RNAi on centrosome number. Many cells showed more than two pericentrin- or γ-tubulin–positive spots (24 ± 1 vs. 8 ± 1% for scrambled control), virtually all of

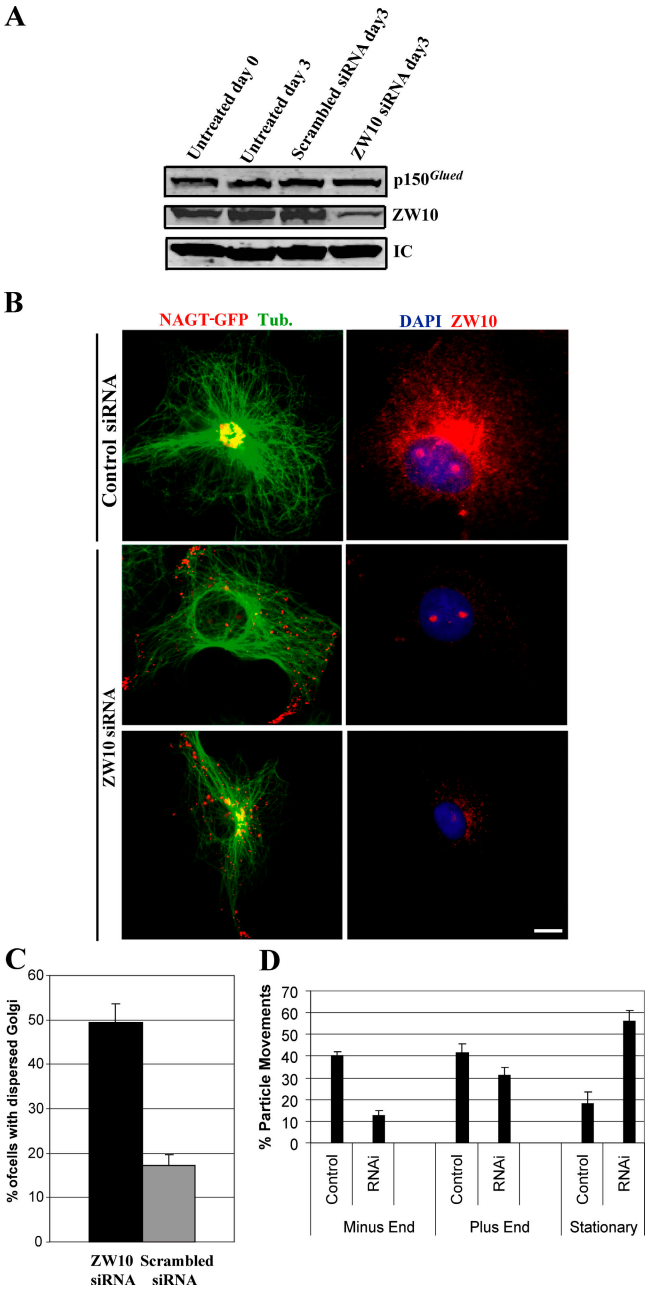

Figure 2. **ZW10 RNAi disperses the Golgi apparatus.** (A) Western blot analysis of total lysates of untreated, ZW10, or scrambled siRNA–transfected COS7 cells after 3 d. ZW10 was dramatically reduced, with no apparent effect on dynein and dynactin levels. (B) Quadruple labeling of ZW10 siRNA–transfected cells showing NAGT-GFP and tubulin (left, red and green, respectively), and ZW10 and DAPI (right, red and blue, respectively). ZW10 RNAi causes a clear reduction in ZW10 staining intensity and pronounced Golgi dispersal, relative to the scrambled siRNA control. Microtubules are disrupted in many cells (middle), but are radially organized in others in which the Golgi apparatus is still dispersed. (C) Quantitative analysis of Golgi dispersal in ZW10 siRNA– or control siRNA–transfected cells. Values are means ± SD from three independent experiments. $n = 150$ cells in each case. (D) Quantification of Golgi movements. ZW10 RNAi caused a clear decrease in microtubule minus end–directed Golgi movements. A smaller decrease in microtubule plus end–directed movements is also seen, along with a substantial increase in stationary Golgi particles. $P < 0.02$; *t* test. Values are means ± SD from three independent control and experimental videos. $n = 100$ particles in each case. Bar, 5 μm.

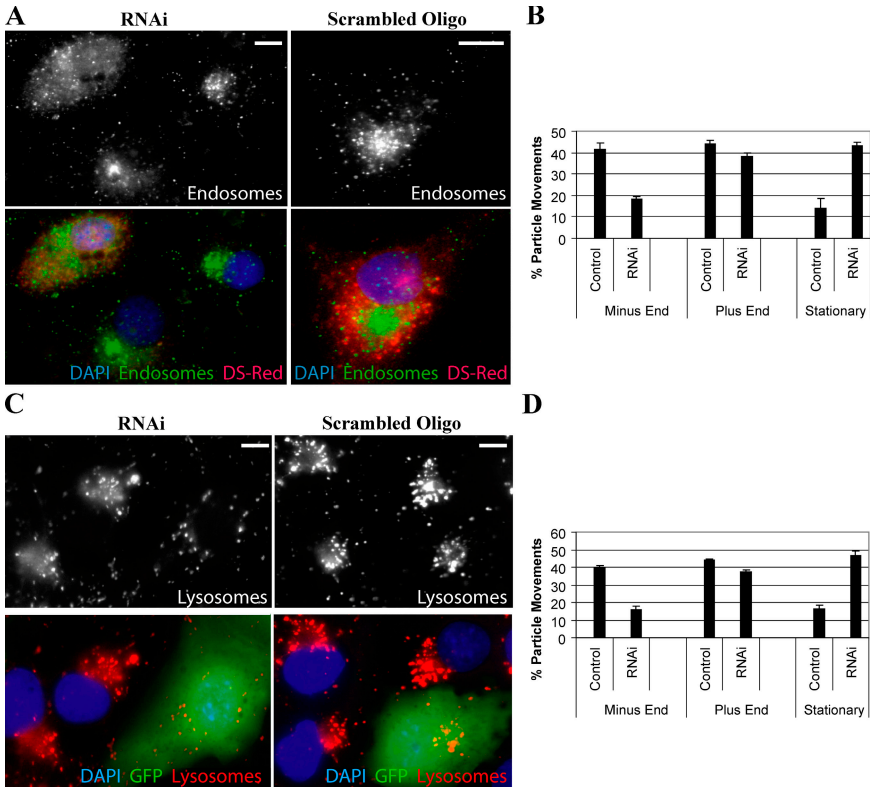

Figure 3. **Effect of ZW10 RNAi on endosome and lysosome motility.** (A) COS-7 cells triply labeled with FITC-transferrin (green), DAPI (blue), and DS-Red (red) as transfection markers show dispersal of endosomes. (B) Quantitation of endosome (TRITC-Tf marker) motility visualized by live imaging of cells transfected with GFP-tubulin and either ZW10 siRNA or scrambled control. $P < 0.02$; *t* test. Values are means ± SD from three independent control and experimental videos. $n = 50$ particles chosen in a designated rectangular region within the imaged cell in each case. (C) COS-7 cells triply labeled with LysoTracker red (red), Hoechst (blue), and GFP (green) as transfection markers show dispersal of lysosomes. (D) Quantitation of lysosome (LysoTracker red marker) motility visualized by live imaging of cells transfected with GFP-tubulin and either siRNA or scrambled control. Effects of ZW10 RNAi on endosome and lysosome motility were strikingly similar to those observed for Golgi elements in Fig. 2 D. $P < 0.02$; *t* test. Values are means ± SD from three independent control and experimental videos. $n = 50$ particles chosen in a designated rectangular region within the imaged cell in each case. Bars, 5 μm.

which contained centrioles, as revealed by staining with the GT335 anti–polyglutamyl-tubulin antibody. However, microtubules were disorganized in a much greater fraction of cells (80%), suggesting that ZW10 also plays a more direct role in localizing microtubule nucleating or assembly factors.

Effects of ZW10 RNAi on membrane motility

The disruption of the Golgi apparatus by multiple means strongly supports a role for ZW10 in controlling Golgi organization. A previous study attributed similar phenotypic effects to a SNARE-related mechanism (Hirose et al., 2004), despite ZW10's known role in mitotic dynein function (Starr et al., 1998). To test directly for a role for ZW10 in interphase dynein function, we conducted live imaging of Golgi vesicles in cells subjected to ZW10 RNAi. To ensure proper scoring of minus end– versus plus end–directed movement, we coexpressed YFP-tubulin along with the RNAi. Only cells in which a clear radial microtubule organization persisted were included in this analysis (Videos 1 and 2, available at http://www.jcb.org/cgi/content/full/jcb.200510120/DC1). As in the fixed images, Golgi elements labeled with NAGT-GFP were dispersed by ZW10 RNAi. Analysis of vesicle movements revealed an ∼70% decrease in the number of minus end–directed movements, relative to results obtained using a scrambled control (Fig. 2 D). Plus end–directed movements were also reduced, but this effect was much smaller. This result is reminiscent of recent observations of the effects of dynamitin overexpression in frog melanophores, where it was attributed to a role for dynactin in the anchoring of kinesins, as well as dynein, to vesicular organelles (Blangy et al., 1997; Deacon et al., 2003). A pronounced increase in the percentage of stationary NAGT-GFP vesicles was also observed (Fig. 2 D).

To determine whether other minus end–directed membranous structures were also affected by ZW10 RNAi, we examined cells expressing YFP-tubulin and labeled with either the endosomal marker FITC-Tf or the lysosomal marker LysoTracker red. Vesicular elements labeled with each marker were dispersed as revealed by both immunocytochemistry and live imaging (Fig. 3, A and C). Analysis of vesicle motility (Videos 3–6, available at http://www.jcb.org/cgi/content/full/jcb.200510120/DC1) again revealed a clear decrease in minus end–directed movements that was comparable in magnitude to that observed for Golgi elements, a similar smaller decrease in plus end–directed movements, and a substantial increase in stationary particles (Fig. 3, B and D).

Effect of RNAi on dynein targeting

To test for a role for ZW10 in anchoring dynein to membranous organelles, we stained HeLa cells subjected to ZW10 RNAi with an antibody specific for Golgi cytoplasmic dynein heavy chain that was reported for cells overexpressing the dynactin subunit dynamitin (Roghi and Allan, 1999). Dynein staining at the Golgi apparatus was also reduced by ZW10 RNAi (Fig. 4, A and B). Vector-based ZW10 RNAi (Fig. 4 A, bottom) reduced Golgi-associated dynein immunofluorescence almost completely. In contrast, the dominant-inhibitory HZW10-4 cDNA had little detectable effect on Golgi dynein heavy chain staining (not depicted). This result suggests that HZW10-4 produces its inhibitory effects by a means independent of dynein targeting.

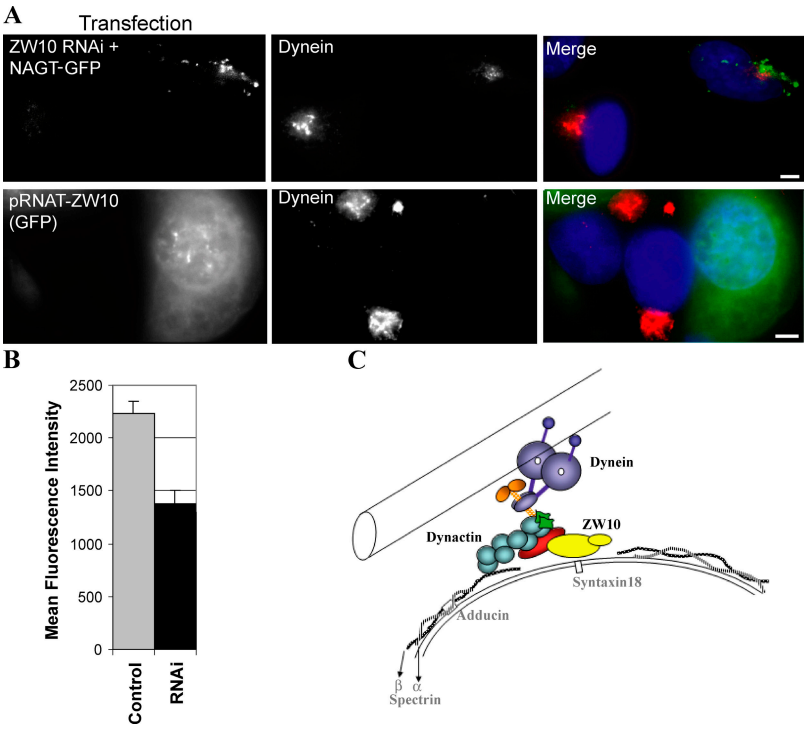

Figure 4. **Effect of ZW10 RNAi on association of dynein with Golgi membranes.** HeLa cells were subjected to ZW10 RNAi, and Golgi-associated dynein was visualized using a Golgi-specific cytoplasmic dynein heavy chain antibody. (A) Cells were transfected with ZW10 siRNA and NAGT-GFP (top) or with a cDNA encoding a ZW10 shRNA plus GFP (bottom). (B) Quantitative analysis of dynein heavy chain immunofluorescence. Data are from siRNA-transfected versus scrambled control–transfected cells from experiment shown in top of A. Values are means ± SD from $n = 10$ experimental and $n = 10$ control cells and represent total cellular Golgi dynein fluorescence. $P < 0.01$; *t* test. (C) Schematic representation of ZW10 membrane interactions. The ZW10 complex is shown in yellow associated with the dynamitin subunit (red) of the dynactin complex, which in turn anchors cytoplasmic dynein. The relationship between this model and evidence of a role for Golgi spectrin in dynein anchoring is uncertain. However, because ZW10 and spectrin interact with distinct dynactin subunits (dynamitin and Arp1, respectively), the two modes of attachment are not mutually exclusive. The ZW10 complex also interacts with the t-SNARE synataxin-18, but whether this interaction plays a role in dynein targeting is unknown. Bars, 5 μm.

In support of this possibility, HZW10-4 failed to displace dynein and dynactin from kinetochores (unpublished data), despite a pronounced effect on mitotic progression (see Inhibition of ZW10 function).

HZW10-4 appears to contain part of, but not the entire, interaction region for the dynactin subunit dynamitin (Starr et al., 1998). Although we observed coimmunoprecipitation of overexpressed dynamitin with full-length ZW10, we have not detected an interaction between dynamitin and the HZW10-4 fragment in this assay or by sucrose density gradient centrifugation of HZW10-4–transfected cell lysates (McKenney, R., personal communication). The fragment could be detected at kinetochores (unpublished data). However, the persistence of dynein at this site and at the Golgi apparatus argues against a role for the corresponding ZW10 domain in dynein targeting. Instead, these data suggest additional roles for ZW10 or its interacting proteins in mitotic checkpoint and dynein motor regulation. This fragment seems to differ in its phenotypic effects from an NH_2-terminal fragment reported to interfere with ER–Golgi trafficking (Hirose et al., 2004). The latter was reported to interact with the t-SNARE syntaxin-18, suggesting a role for ZW10 in membrane budding and fusion. Therefore, ZW10 conceivably participates both in syntaxin-18–mediated membrane sorting and in dynein-mediated membrane transport, though some of the earlier data could be dynein related. A key finding of that study was a ZW10-associated defect in vesicular stomatitis virus glycoprotein trafficking, a classic indicator of ER–Golgi sorting, though this process was delayed rather than blocked. Because transport of the ER–Golgi intermediate compartment vesicles is under dynein control (Burkhardt et al., 1997; Presley et al., 1997), a delay in trafficking could conceivably result from a transport, rather than a trafficking, defect.

Cortical association of ZW10

During interphase, cytoplasmic dynein associates with the cortex of migrating cells and can be seen prominently at the leading cell edge (Dujardin et al., 2003). In view of the expanded range of dynein-related functions in which our data now implicate ZW10, we tested further for its distribution in migrating cells (Fig. 5). ZW10 immunoreactivity was observed in a pattern strikingly similar to that of cytoplasmic dynein, which is associated with the leading cell edge in advance of most of the microtubules in the region.

Models for interphase role of ZW10

This study provides the first evidence for an association of ZW10 with Golgi elements in particular and for a general role in interphase cytoplasmic dynein function. Furthermore, it strongly suggests that ZW10 serves a role during interphase related to that at the kinetochore, i.e., at least in part as an anchor for dynein and dynactin. In light of the reported interaction between ZW10 and dynamitin (Starr et al., 1998), we anticipate a comparable hierarchy of interactions at the surface of Golgi elements, as well as of endosomes and lysosomes (Fig. 4 C).

An important issue is how this model relates to the role proposed for the spectrin cytoskeleton in dynein targeting (Holleran et al., 1996; Muresan et al., 2001). As seen in Fig. 4 C, the two models are not mutually exclusive. A Golgi-associated spectrin isoform, βIII spectrin, was found to bind to the Arp1 subunit of dynactin (Holleran et al., 1996, 2001), whereas ZW10 binds to the dynamitin subunit (Starr et al., 1998). Thus, it is possible that dynactin has two distinct interaction partners at the Golgi surface, which could function in concert. Based on this study, ZW10 appears to be necessary for normal binding.

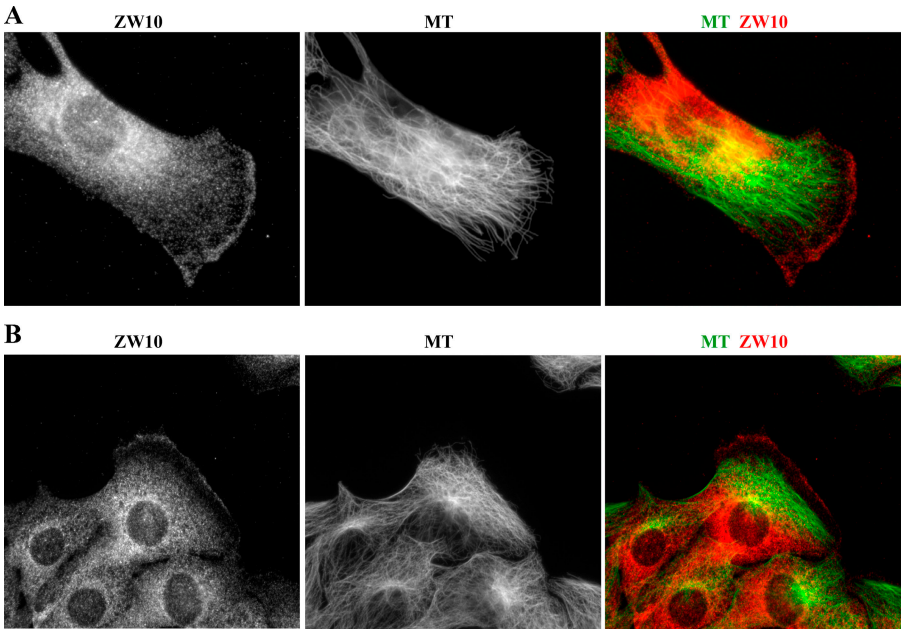

Figure 5. **Association of ZW10 with leading edge of migrating fibroblasts.** NIH3T3 cells were plated at low density or grown to confluence, wounded, and processed for immunostaining after 2 h recovery in the presence of serum. Double labeling with anti-ZW10 (red) and anti-tubulin (green) revealed an association of ZW10 with the lamellipodial leading edge in freely migrating (A) and wounded cultures (B).

Its contribution relative to that of the spectrin-mediated mechanism remains to be fully assessed.

How ZW10 itself binds to membranes is unknown. This interaction could, conceivably, involve syntaxin-18. Immunoprecipitates of this protein were found to contain ZW10; RINT-1, which is a protein first identified in the Rad50 DNA repair pathway; and p31, another SNARE-related protein (Hirose et al., 2004). It is now known that ZW10 and RINT-1 exist as a complex (Hirose et. al., 2004; Kops et al., 2005) and that both proteins, along with p31, are released from syntaxin-18 by α−SNAP in the presence of ATP (Hirose et. al., 2004). How these results, and the lack of a direct interaction between ZW10 or RINT-1 with syntaxin-18, may relate to dynein targeting remains to be explored. Rab6 (Short et al., 2002) and *lava lamp* (Papoulas et al., 2005) have also been implicated in Golgi dynein targeting. Whether ZW10 functions in concert with these proteins or independently is unclear.

It is appealing to speculate, as a final consideration, that other features of the interaction of ZW10 with kinetochore pertain to its association with cellular membranes. ZW10-interacting protein-1, for example, has been identified as an upstream interactor for ZW10 at kinetochores (Wang et al., 2004; Kops et al., 2005). Whether ZW10-interacting protein-1 itself or some other yet to be identified protein serve in this capacity during interphase remains an important question for further investigation.

Finally, we note that our observation of ZW10 at the leading edge of migrating cells provides a potentially valuable clue to the mechanisms of the, until now, mysterious recruitment to and association with dynein to the lamellipodial cortex.

Materials and methods

Plasmids

Full-length HZW10 (Starr et al., 1997) was inserted into the pcDNA3.1 vector (Invitrogen) using the BamHI and XhoI restriction sites. A myc tag was inserted at the 5′ end of each HZW10 fragment (Fig. S1 A) using the same restriction sites and plasmid vector. pCNG2, encoding a GFP-,β1, 2*N*-acetylglucosaminyltransferase I (NAGT-GFP) fusion protein, was a gift from D. Shima and G. Warren (Imperial Cancer Research Fund, London, UK). β-Galactosidase overexpression was performed using pCMVβ vector (CLONTECH Laboratories, Inc).

Antibodies

The polyclonal antibody anti-HZW10 was previously described elsewhere (Starr et al., 1997). A polyclonal antibody termed anti-Cter was raised against the 23 COOH-terminal amino acids of HZW10 (Research Genetics). This peptide, coupled to a cyanogen bromide–activated Sepharose 4B column, was used to affinity purify anti-Cter, and the antibodies were eluted with a pH2–pH5 gradient of glycine/HCl (Research Genetics).

Monoclonal anti-p150^{Glued} and anti-GM130 antibodies were obtained from BD Biosciences. Polyclonal Golgi-specific anti-dynein heavy chain (Roghi and Allan, 1999) was a gift from V. Allan (University of Manchester, Manchester, UK). Monoclonal antibodies directed against the Golgi markers 58K, γ-adaptin, β-COP, and α-tubulin (clone DM1A) were purchased from Sigma-Aldrich. Polyclonal anti–β-gal antibody was obtained from US Biological.

Cell culture

COS-7 and HeLa cells were grown in DMEM with 10% fetal calf serum supplemented with 100 U/ml penicillin and 100 mg/ml streptomycin. NIH3T3 cells were grown in DMEM with 10% bovine calf serum, and wound-healing assays were performed as previously described (Dujardin et al., 2003). For microinjection, the affinity-purified antibody was dialyzed overnight into microinjection buffer (50 mM potassium glutamate and 0.5 mM $MgCl_2$, pH 7.0) and concentrated to 6.8 mg/ml. Cells were fixed 6 h after injection. Microinjection was performed using a micromanipulator (model 5171; Eppendorf) coupled to a microscope (model DMIRBE; Leica). siRNA were prepared and introduced into COS7 cells according to the specifications of the manufacturer (Dharmacon RNA Technologies). The RNA sequences used were AAGGGUGAGGUGUGCAAUAUG, for ZW10 siRNA, and AUUGUAUGCGAUCGCAGACUU, for a scrambled negative control. We also designed a pRNAT-ZW10 cDNA (pRNAT-U6.1/Neo), which encodes an shRNA corresponding to a distinct ZW10 target sequence (CGGTGAATTTACAGACTTAAA), as well as GFP (GenScript Corp.).

Biochemical methods

To test for anti-Cter ZW10 peptide antibody specificity (Fig. 1 A), cells were rinsed in ice-cold PBS (137 mM NaCl, 2.7 mM KCl, 8.1 mM Na_2HPO_4, and 1.5 mM KH_2PO_4, pH 7.4) and harvested in 150 mM NaCl, 10 mM Tris, pH 7.2, 1% deoxycholate, 1% Triton X-100, and 0.1% SDS containing a protease inhibitor mixture (2 μg/ml each of aprotinin

and leupeptin, 1 mM EGTA, and 1 mM 4-(2-aminoethyl)benzenesulphonyl fluoride). After incubation on ice for 20 min, the cell lysate was spun for 10 min at 13,000 *g*, and the supernatant was subjected to SDS-PAGE and Western blotting. For immunoprecipitation, cells were extracted in 150 mM NaCl, 50 mM Tris, pH 8.0, 1% NP-40, and protease inhibitors.

Membrane flotation in a discontinuous 2/1.6/1.4/1.2/0.8 M sucrose gradient was conducted as described (Balch et al., 1984). 1-ml fractions were collected from the bottom of the gradient and analyzed by Western blotting. Each fraction was also diluted in 150 mM NaCl and 50 mM Tris, pH 8.0. Membranes were sedimented at 15,000 *g* for 15 min and solubilized by adding 1% Triton X-100. Direct membrane sedimentation tests on Dounce-homogenized total cell extract were also performed at 15, 000 *g* for 15 min.

Immunofluorescence microscopy and live-cell imaging

For Golgi staining, cells were rinsed in PBS and fixed for 6 min at −20°C in methanol. For costaining of Golgi and microtubules after ZW10 antibody injection, cells were rinsed in PHEM buffer (120 mM Pipes, 50 mM Hepes, 20 mM EGTA, and 4 mM magnesium acetate, pH 6.9) and fixed for 6 min at −20°C in methanol. Sequential antibody incubations were used because both GM130 and α-tubulin antibodies were monoclonal. To determine the mitotic index, cells were rinsed in PHEM buffer and fixed in 4% paraformaldehyde, 0.05% glutaraldehyde, and 0.05% Triton X-100 for 12 min. Cells were then permeabilized for 25 min in 0.5% Triton X-100 in PBS, and incubated twice for 10 min in PBS containing 10 mg/ml $NaBH_4$. 0.05% saponin was added for ZW10 Golgi staining. Images were obtained using a DMIRBE microscope equipped with a camera (ORCA 100; Hamamatsu) and Metamorph software (Universal Imaging Corp.). Z-series stacks were acquired with 0.3-μm steps; the out of focus signal was reduced using Metamorph 2D deconvolution, and the final images were obtained by total projection of the image stacks. Confocal microscopy was performed with a microscope (Diaphot 200; Nikon) coupled to a system (MRC1000; Bio-Rad Laboratories) equipped with a Kr/Ar laser (MRC1000; Bio-Rad Laboratories).

For live-cell imaging of Golgi, COS7 cells were cotransfected with NAGT-GFP and tubulin-YFP constructs, along with ZW10 siRNA or control oligonucleotide treatment, for 3 d. For live imaging of endosomes, cells cotransfected with tubulin-GFP and ZW10 RNAi or control oligonucleotide were treated with TRITC-transferrin for 1 h before obtaining the time-lapse images. Cells were treated with LysoTracker red for 2 h to visualize lysosomes in live cells transfected with tubulin-GFP and ZW10 siRNA or control oligonucleotide. Time-lapse images were acquired at 37°C every 1 s for a period of 2 min (1.5 min for endosomes) using a DMIRBE microscope equipped with an incubation chamber for temperature and CO_2 control.

All images were visualized using either a PLAN APO 63×,1.23 NA, or C PLAN 100×, 1.25 NA, oil-immersion objective lenses (Leica).

Online supplemental material

Figs. S1 and S2 show the effects of dominant-negative ZW10 cDNA expression and anti-ZW10 antibody injection on Golgi organization in COS7 cells. Videos show the effect of ZW10 RNAi on Golgi (Videos 1 and 2), endosome (Videos 3 and 4), and lysosome (Videos 5 and 6) motility in control oligonucleotide versus siRNA-transfected cells. Online supplemental material is available at http://www.jcb.org/cgi/content/full/jcb.200510120/DC1.

We thank M. Goldberg for reagents and extensive advice; R. McKenney for help with biochemistry; Dr. V. Allan for anti-dynein heavy chain antibody; Dr. P. Denoulet for the GT335 antibody; and Drs. J. Burkhardt, Y. Argon, and B. Lauring for helpful advice.

This work was supported by National Institutes of Health grant GM47434 (R.B. Vallee) and the Human Frontier Science Program (D. Dujardin).

Submitted: 25 October 2005
Accepted: 22 January 2006

References

Balch, W.E., W.G. Dunphy, W.A. Braell, and J.E. Rothman. 1984. Reconstitution of the transport of protein between successive compartments of the Golgi measured by the coupled incorporation of *N*-acetylglucosamine. *Cell*. 39:405–416.

Basto, R., R. Gomes, and R.E. Karess. 2000. Rough deal and Zw10 are required for the metaphase checkpoint in *Drosophila*. *Nat. Cell Biol.* 2:939–943.

Blangy, A., L. Arnaud, and E.A. Nigg. 1997. Phosphorylation by p34cdc2 protein kinase regulates binding of the kinesin-related motor HsEg5 to the dynactin subunit p150. *J. Biol. Chem.* 272:19418–19424.

Burkhardt, J.K., C.J. Echeverri, T. Nilsson, and R.B. Vallee. 1997. Overexpression of the dynamitin (p50) subunit of the dynactin complex disrupts dynein-dependent maintenance of membrane organelle distribution. *J. Cell Biol.* 139:469–484.

Chan, G.K., S.A. Jablonski, D.A. Starr, M.L. Goldberg, and T.J. Yen. 2000. Human Zw10 and ROD are mitotic checkpoint proteins that bind to kinetochores. *Nat. Cell Biol.* 2:944–947.

Deacon, S.W., A.S. Serpinskaya, P.S. Vaughan, M. Lopez Fanarraga, I. Vernos, K.T. Vaughan, and V.I. Gelfand. 2003. Dynactin is required for bidirectional organelle transport. *J. Cell Biol.* 160:297–301.

Dujardin, D.L., L.E. Barnhart, S.A. Stehman, E.R. Gomes, G.G. Gundersen, and R.B. Vallee. 2003. A role for cytoplasmic dynein and LIS1 in directed cell movement. *J. Cell Biol.* 163:1205–1211.

Echeverri, C.J., B.M. Paschal, K.T. Vaughan, and R.B. Vallee. 1996. Molecular characterization of the 50-kD subunit of dynactin reveals function for the complex in chromosome alignment and spindle organization during mitosis. *J. Cell Biol.* 132:617–633.

Hirose, H., K. Arasaki, N. Dohmae, K. Takio, K. Hatsuzawa, M. Nagahama, K. Tani, A. Yamamoto, M. Tohyama, and M. Tagaya. 2004. Implication of ZW10 in membrane trafficking between the endoplasmic reticulum and Golgi. *EMBO J.* 23:1267–1278.

Holleran, E.A., M.K. Tokito, S. Karki, and E.L. Holzbaur. 1996. Centractin (ARP1) associates with spectrin revealing a potential mechanism to link dynactin to intracellular organelles. *J. Cell Biol.* 135:1815–1829.

Holleran, E.A., L.A. Ligon, M. Tokito, M.C. Stankewich, J.S. Morrow, and E.L. Holzbaur. 2001. beta III spectrin binds to the Arp1 subunit of dynactin. *J. Biol. Chem.* 276:36598–36605.

Howell, B.J., B.F. McEwen, J.C. Canman, D.B. Hoffman, E.M. Farrar, C.L. Rieder, and E.D. Salmon. 2001. Cytoplasmic dynein/dynactin drives kinetochore protein transport to the spindle poles and has a role in mitotic spindle checkpoint inactivation. *J. Cell Biol.* 155:1159–1172.

Karess, R. 2005. Rod-Zw10-Zwilch: a key player in the spindle checkpoint. *Trends Cell Biol.* 15:386–392.

Kops, G.J., Y. Kim, B.A. Weaver, Y. Mao, I. McLeod, J.R. Yates III, M. Tagaya, and D.W. Cleveland. 2005. ZW10 links mitotic checkpoint signaling to the structural kinetochore. *J. Cell Biol.* 169:49–60.

Muresan, V., M.C. Stankewich, W. Steffen, J.S. Morrow, E.L. Holzbaur, and B.J. Schnapp. 2001. Dynactin-dependent, dynein-driven vesicle transport in the absence of membrane proteins: a role for spectrin and acidic phospholipids. *Mol. Cell*. 7:173–183.

Papoulas, O., T.S. Hays, and J.C. Sisson. 2005. The golgin Lava lamp mediates dynein-based Golgi movements during *Drosophila* cellularization. *Nat. Cell Biol.* 7:612–618.

Presley, J.F., N.B. Cole, T.A. Schroer, K. Hirschberg, K.J. Zaal, and J. Lippincott-Schwartz. 1997. ER-to-Golgi transport visualized in living cells. *Nature*. 389:81–85.

Quintyne, N.J., S.R. Gill, D.M. Eckley, C.L. Crego, D.A. Compton, and T.A. Schroer. 1999. Dynactin is required for microtubule anchoring at centrosomes. *J. Cell Biol.* 147:321–334.

Roghi, C., and V.J. Allan. 1999. Dynamic association of cytoplasmic dynein heavy chain 1a with the Golgi apparatus and intermediate compartment. *J. Cell Sci.* 112:4673–4685.

Savoian, M.S., M.L. Goldberg, and C.L. Rieder. 2000. The rate of poleward chromosome motion is attenuated in Drosophila zw10 and rod mutants. *Nat. Cell Biol.* 2:948–952.

Scaerou, F., I. Aguilera, R. Saunders, N. Kane, L. Blottiere, and R. Karess. 1999. The rough deal protein is a new kinetochore component required for accurate chromosome segregation in *Drosophila*. *J. Cell Sci.* 112:3757–3768.

Scaerou, F., D.A. Starr, F. Piano, O. Papoulas, R.E. Karess, and M.L. Goldberg. 2001. The ZW10 and Rough Deal checkpoint proteins function together in a large, evolutionarily conserved complex targeted to the kinetochore. *J. Cell Sci.* 114:3103–3114.

Short, B., C. Preisinger, J. Schaletzky, R. Kopajtich, and F.A. Barr. 2002. The Rab6 GTPase regulates recruitment of the dynactin complex to Golgi membranes. *Curr. Biol.* 12:1792–1795.

Starr, D.A., B.C. Williams, Z. Li, B. Etemad-Moghadam, R.K. Dawe, and M.L. Goldberg. 1997. Conservation of the centromere/kinetochore protein ZW10. *J. Cell Biol.* 138:1289–1301.

Starr, D.A., B.C. Williams, T.S. Hays, and M.L. Goldberg. 1998. ZW10 helps recruit dynactin and dynein to the kinetochore. *J. Cell Biol.* 142:763–774.

Tai, C.Y., D.L. Dujardin, N.E. Faulkner, and R.B. Vallee. 2002. Role of dynein, dynactin, and CLIP-170 interactions in LIS1 kinetochore function. *J. Cell Biol.* 156:959–968.

Vallee, R.B., J.C. Williams, D. Varma, and L.E. Barnhart. 2004. Dynein: an ancient motor protein involved in multiple modes of transport. *J. Neurobiol.* 58:189–200.

Wang, H., X. Hu, X. Ding, Z. Dou, Z. Yang, A.W. Shaw, M. Teng, D.W. Cleveland, M.L. Goldberg, L. Niu, and X. Yao. 2004. Human Zwint-1 specifies localization of Zeste White 10 to kinetochores and is essential for mitotic checkpoint signaling. *J. Biol. Chem.* 279:54590–54598.

Williams, B.C., T.L. Karr, J.M. Montgomery, and M.L. Goldberg. 1992. The *Drosophila l*(1)*zw10* gene product, required for accurate mitotic chromosome segregation, is redistributed at anaphase onset. *J. Cell Biol.* 118:759–773.

Williams, B.C., S. Liu, Z.-X. Li, E.V. Williams, G. Leung, T.J. Yen, and M.L. Goldberg. 2003. Zwilch, a new component of the ZW10/ROD complex required for kinetochore functions. *Mol. Biol. Cell*. 14:1379–1391.

Wojcik, E., R. Basto, M. Serr, F. Scaerou, R. Karess, and T. Hays. 2001. Kinetochore dynein: its dynamics and role in the transport of the rough deal checkpoint protein. *Nat. Cell Biol.* 3:1001–1007.